

Article

Single-Cell Screening through Cell Encapsulation in Photopolymerized Gelatin Methacryloyl

Venkatesh Kumar Panneer Selvam ¹, Takeru Fukunaga ¹, Yuya Suzuki ¹, Shunya Okamoto ¹, Takayuki Shibata ¹, Tuhin Subhra Santra ² and Moeto Nagai ^{1,3,*}

¹ Department of Mechanical Engineering, Toyohashi University of Technology, 1-1 Hibarigaoka, Tenpaku-cho, Toyohashi 444-8580, Japan; venkatesh.kumar.panneer.selvam.rx@tut.jp (V.K.P.S.); fukunaga.takeru.sq@tut.jp (T.F.); suzuki.yuya.kz@tut.jp (Y.S.); okamoto@me.tut.ac.jp (S.O.); shibata@me.tut.ac.jp (T.S.)

² Department of Engineering Design, Indian Institute of Technology Madras, Chennai 600036, India; tuhin@iitm.ac.in

³ Institute for Research on Next-Generation Semiconductor and Sensing Science, Toyohashi University of Technology, 1-1 Hibarigaoka, Tenpaku-cho, Toyohashi 444-8580, Japan

* Correspondence: nagai@me.tut.ac.jp; Tel.: +81-532-44-6701

Abstract: This study evaluated the potential of gelatin methacryloyl (GelMA) for single-cell screening compared to polyethylene glycol diacrylate (PEGDA). GelMA photopolymerized at 1000–2000 mJ/cm² produced consistent patterns and supported HeLa cell viability. GelMA (5%w/v) facilitated better cell collection within 2 days due to its shape retention. GelMA demonstrated biocompatibility with HeLa cells exhibiting exponential proliferation and biodegradation over 5 days. The average cell displacement over 2 days was 16 μm. Two targeted cell recovery strategies using trypsin were developed: one for adherent cells encapsulated at 800 mJ/cm², and another for floating cells encapsulated at 800 mJ/cm², enabling the selective removal of unwanted cells. These findings suggest GelMA as a promising biomaterial for single-cell screening applications, offering advantages over PEGDA in cell encapsulation and targeted recovery.

Keywords: GelMA; long-term viability; biodegradability; photopolymerization; cell screening



Citation: Panneer Selvam, V.K.; Fukunaga, T.; Suzuki, Y.; Okamoto, S.; Shibata, T.; Santra, T.S.; Nagai, M. Single-Cell Screening through Cell Encapsulation in Photopolymerized Gelatin Methacryloyl. *Micro* **2024**, *4*, 295–304. <https://doi.org/10.3390/micro4020018>

Academic Editor: Laura Chronopoulou

Received: 25 February 2024

Revised: 8 April 2024

Accepted: 25 April 2024

Published: 27 April 2024



Copyright: © 2024 by the authors. Licensee MDPI, Basel, Switzerland. This article is an open access article distributed under the terms and conditions of the Creative Commons Attribution (CC BY) license (<https://creativecommons.org/licenses/by/4.0/>).

1. Introduction

Single-cell screening is a crucial technique for collecting specific cells based on the desired characteristics [1–3]. A major method for obtaining target cell populations is flow cytometric cell sorting [4,5], which is based on the optical and fluorescent characteristics of individual cells [6,7]. During flow cytometry, suspended cells pass through a detector in a short period of time. It is important to note that flow cytometry has inherently limited measurement quality.

Image-based single-cell screening systems overcome these limitations by utilizing high-resolution imaging and temporal analysis, allowing for the detection of weak signals and transient events [8]. This approach offers flexible cell collection methods, including single-pipette [9,10] and laser-based techniques [11]. Collected cells, both of interest [12–14] or not [15], can be encapsulated in photopolymerizable hydrogels like polyethylene glycol diacrylate (PEGDA) using light irradiation. Although the number of target cells is often greater than unwanted cells, and encapsulating cells of interest in PEGDA hydrogels is relatively straightforward, encapsulating negative cells is less efficient. While PEGDA hydrogels are suitable for DNA extraction, they have limitations such as slow degradation [16] and cytotoxicity at lower molecular weights [17,18]. For viable cell recovery and subsequent analysis, the surrounding hydrogel needs to degrade.

Gelatin methacrylate (GelMA) offers distinct advantages. This biocompatible material degrades by both cells and enzymes [19–21], making it more suitable for cell screening

via encapsulation than PEGDA. The long-term viability of cells encapsulated in GelMA micromodules [22] and microspheres [23,24] has been established. Cells were acoustically patterned into diverse arrangements and encapsulated in GelMA for applications such as studying stem cell differentiation [25], constructing heterogeneous tissue models [26], and high-throughput drug testing [27]. GelMA hydrogels can be degraded using readily available enzymes like trypsin [28] and collagenase [29,30], facilitating efficient cell collection. While we have developed an automated single-cell encapsulation system [31], the specific properties of GelMA in the context of single-cell screening and the efficient collection of target cells after encapsulation remain unexplored.

To address this gap, we investigated the effects of GelMA hydrogels on cell proliferation, biodegradation, and cell motility within the gels for target single-cell collection. We tested both suspended and adherent cells for collecting cells encapsulated in GelMA. Our study successfully demonstrates the recovery of single floating and adherent cells through gel lysis using a time-controlled trypsin treatment.

2. Materials and Methods

2.1. Bioink and Cells

GelMA bioink was prepared by filling a centrifuge tube with 2 mL of phosphate-buffered saline (PBS(-), Gibco Ltd., pH 7.4, 1×, Newington, NH, USA). Cytotoxicity depends on the concentration of photopolymerized hydrogel during encapsulation [32,33]. We reduced the concentration of GelMA to 5%*w/v*. Of the GelMA (Sigma Aldrich, Saint Louis, MO, USA, gelatin methacryloyl, 900628, with a gel strength of 90–110 g Bloom and a degree of substitution of 60%), 0.1 g was added to the same tube, creating a 5%*w/v* GelMA solution in PBS(-). The GelMA solution was mixed with 10 mg of LAP (Lithium Phenyl(2,4,6-trimethylbenzoyl)phosphinate, LAP, L0290, Tokyo Kasei Kogyo Co., Ltd., Tokyo, Japan). The final concentration of LAP was 0.5%*w/v* in PBS(-).

HeLa cells (RCB0007, RIKEN BRC, Wako, Japan) were cultured in minimum essential media (MEM) supplemented with 10% fetal bovine serum (FBS) and 1% penicillin–streptomycin (Pen/Strep). The culture medium was removed, and cells were washed with 3 mL of PBS. Subsequently, 3 mL of 0.25% trypsin–EDTA 1X (Gibco™, 25200072, USA) was added to the dish and incubated for 4 min in a CO₂ incubator. Following incubation, 3 mL of the medium was added to the trypsinized cells, and the suspension was centrifuged for 3 min to remove the supernatant. Finally, the cells were resuspended for subsequent use in either a culture medium or bioink.

2.2. Irradiation Setup

Cuvettes were constructed using four glass substrates (Figure 1a,d,h). The bottom substrate consistently used a glass slide measuring 26 × 76 mm (either S2226 with 1.2–1.5 mm thickness or S1111 with 0.8–1.0 mm thickness, both from Matsunami Glass Co., Ltd. (Osaka, Japan)). The top substrate varied between a simple coverslip (2-176-01, 18 × 18 mm, 0.13–0.17 mm thickness) and a coverslip with grid lines (GC1300, 13 mm diameter, 0.16–0.19 mm thickness, both from Matsunami Glass Co., Ltd.). Two additional coverslips were used as spacers in all cases. The bioink was then injected into the assembled cuvette.

The GelMA bioink was photopolymerized using our DMD-based photoirradiation system, as described previously [31,34]. For cell encapsulation, the GelMA hydrogel and cells were exposed to 405 nm light at 100–300 mW/cm² for an integrated light dose of 600–2000 mJ/cm². The irradiation time ranged from 2 s to 8 s. The light pattern consisted of an arrangement of four squares, each measuring 98 μm. The ambient temperature was maintained at 23 °C throughout the process.

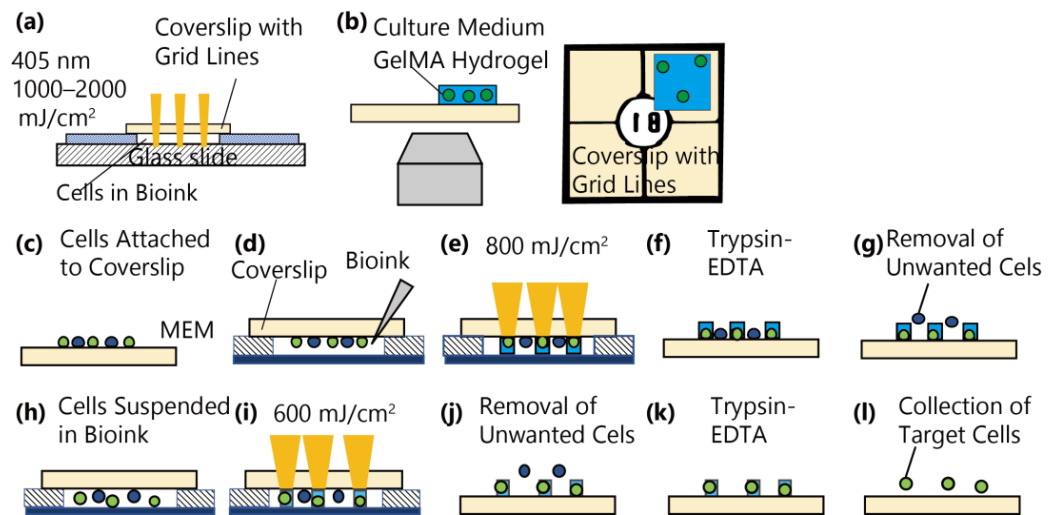


Figure 1. Setup for encapsulating cells in GelMA hydrogels. Green and blue dots are respectively target and unwanted cells. (a,b) Procedure for observing cells in a hydrogel after light irradiation. Blue region is a GelMA hydrogel. (c–g) Selection of target single attached cells encapsulated in GelMA by lysis with trypsin-EDTA. The principle of cell recovery is based on the susceptibility to trypsin. (h–l) Selection of target single suspended cells. The principle of cell selection is based on the susceptibility to flow.

2.3. Live/Dead Assay

Calcein-AM (C396, Dojindo, Tokyo, Japan) (2.0 μM) and 4.0 μM propidium iodide (PI, 341-07881, Dojindo) were prepared in PBS(-). Cell viability was assessed immediately after gel polymerization through light irradiation. Cells were washed with PBS(-) and transferred to a 50 mm Falcon petri dish. Subsequently, 100 μL of the cell staining solution was added to the cells in the dish. To allow for stain diffusion through the gel, the dish was incubated for 35 min at 37 $^{\circ}\text{C}$ and 5% CO_2 in an incubator. For comparison, a cell suspension without photopolymerized gel was also incubated for 15 min as the negative control.

After incubation, the cells were examined under a microscope (Eclipse Ti-U, Nikon, Tokyo, Japan) equipped with a cooled camera (Nikon, DIGITAL SIGHT, DS-Qi1Mc, Tokyo, Japan) using fluorescent filters (B2A: 150 ms, C-FL-C TRITC: 150 ms). Live cells displayed green fluorescence, while dead cells emitted red fluorescence. Cell viability was calculated using the following equation: Cell viability (%) = $N_{\text{Live}} / (N_{\text{Live}} + N_{\text{Dead}})$, where N_{Live} is number of live cells and N_{Dead} is number of dead cells.

2.4. Observation of Cells Encapsulated in GelMA

HeLa cells were encapsulated in GelMA at 1000 mJ/cm^2 and were washed with PBS and cultured in a 50 mm petri dish containing the conditioned medium (MEM supplemented with 10% FBS and 1% Pen/Strep). The dish was kept in an incubator at 37 $^{\circ}\text{C}$ and 5% CO_2 , and observed every day. The encapsulated cells were characterized to observe the cell proliferation, biodegradation of the gel, and cell motility over time. The biodegradability of GelMA was investigated by comparing the gel area after encapsulation by light irradiation. Gels with and without cells were measured for 5 days.

2.5. Encapsulation of Attached and Suspended Cells in GelMA

HeLa cells were encapsulated in GelMA using two strategies: attachment to a coverslip or suspension in a cuvette. Both methods utilized a 40 $\mu\text{m} \times 40 \mu\text{m}$ square pattern for encapsulation. Cells were (1) attached to a coverslip (Figure 1c) or (2) suspended in a cuvette (Figure 1h). These cells were encapsulated in GelMA with a 40 $\mu\text{m} \times 40 \mu\text{m}$ square pattern. We needed more time to detach adherent cells as the GelMA hydrogels were more crosslinked, making degradation take longer. To collect floating cells encapsulated in

GelMA hydrogels, we can ignore cell dissociation and focus on the rapid degradation of GelMA hydrogels with a lower light integral dose of 600 mJ/cm^2 .

(1) A suspension of HeLa cells was incubated for 2 h in a CO_2 incubator at 37°C to promote attachment (Figure 1c). A cuvette was made and $20 \mu\text{L}$ of bioink was injected (Figure 1d). The cuvette with the bioink was placed on the stage of an inverted microscope (Nikon ECLIPSE Ti-U, Tokyo, Japan). HeLa cells were encapsulated on the coverslip within the bioink using 405 nm light with an integral dose of 800 mJ/cm^2 (Figure 1e). (2) HeLa cells were suspended in 2 mL of bioink (Figure 1h). The final concentration of cells was $4 \times 10^6 \text{ cells/mL}$. Single HeLa cells were encapsulated on the coverslip by irradiating the bioink with 405 nm at a light integral of 600 mJ/cm^2 (Figure 1i).

2.6. Collection of Cells with Trypsin

The time-controlled application of trypsin facilitated the selective recovery of encapsulated cells (Figure 1f,g, or Figure 1k,l). The coverslip with encapsulated cells was transferred to a 50 mm Petri dish and rinsed with PBS(-) to remove non-encapsulated cells. Next, trypsin (Gibco Ltd., 0.25% Trypsin-EDTA (1X)) was added to detach adherent cells and degrade the GelMA hydrogel. The exposed cells were detached first, followed by the collection of encapsulated cells after the dissolution of the gel. The dissolution and cell release were monitored using an inverted microscope and a cooled camera.

3. Results and Discussion

3.1. Basic Characterization with GelMA

Figure 2a–e presents the top view of a GelMA hydrogel containing HeLa cells which were irradiated at 1070 mJ/cm^2 to 1920 mJ/cm^2 . The gel was transparent after polymerization of GelMA at a concentration of $5\%w/v$, and the cells encapsulated in the gel were visible. Encapsulating the cells in a thin layer of gel helped maintain their immobilization and viability. Figure 2f depicts the individual gel units, each measuring approximately $92\text{--}94 \mu\text{m}$ after photopolymerization with $98 \mu\text{m}$ square light patterns. In single cell screening, the size of photocured hydrogel is important to determine the limits of the inter space between two patterns. If the size of the pattern is too large or too small compared to the designed values, some margins need to be considered. The data show that within the range of this light integral, the size of the formed hydrogel does not change significantly.

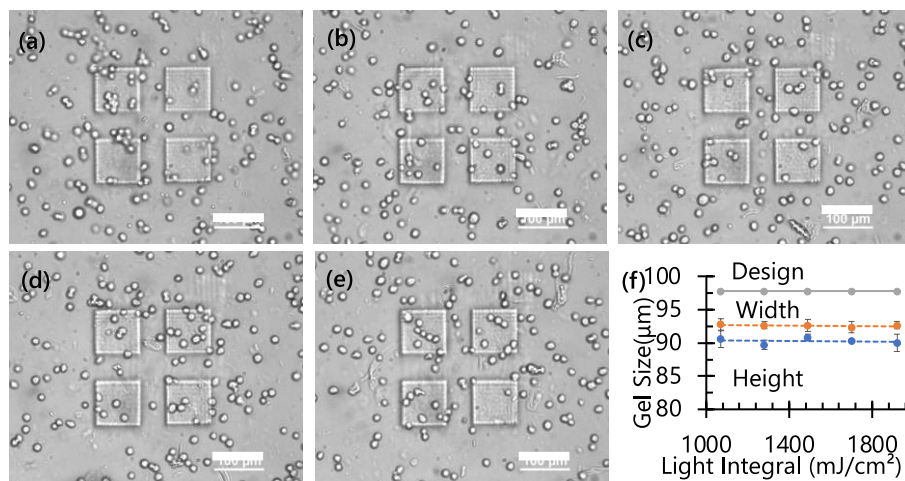


Figure 2. Microscopic images of cured gel at $5\%w/v$ GelMA: (a) 1070 , (b) 1280 , (c) 1490 , (d) 1700 , (e) 1920 mJ/cm^2 . Scale bars: $100 \mu\text{m}$. (f) Height and width of cured hydrogel at different light integral.

Photopolymerized $5\%w/v$ GelMA with encapsulated cells showed high viability of 96% ($43/45$ cells). Ten sites were encapsulated with 1200 mJ/cm^2 light irradiation, and viability was assessed immediately after fluorescence microscopy using Calcein-AM and PI staining. The negative control reached 98% ($173/177$ cells). Figure 3 shows the microscopic

views of cells under different conditions. Figure 3a–c depict cells encapsulated in a 5%w/v GelMA hydrogel that were photopolymerized at 1200 mJ/cm². Figure 3a is a bright field image showing the overall cell population. Figure 3b shows the green fluorescence of live-cell stained with Calcein-AM, indicating viable cells. Figure 3c looks black, suggesting that no dead cells were detected with red fluorescence, stained with PI. Figure 3d–f represents the negative control conditions without any treatment.

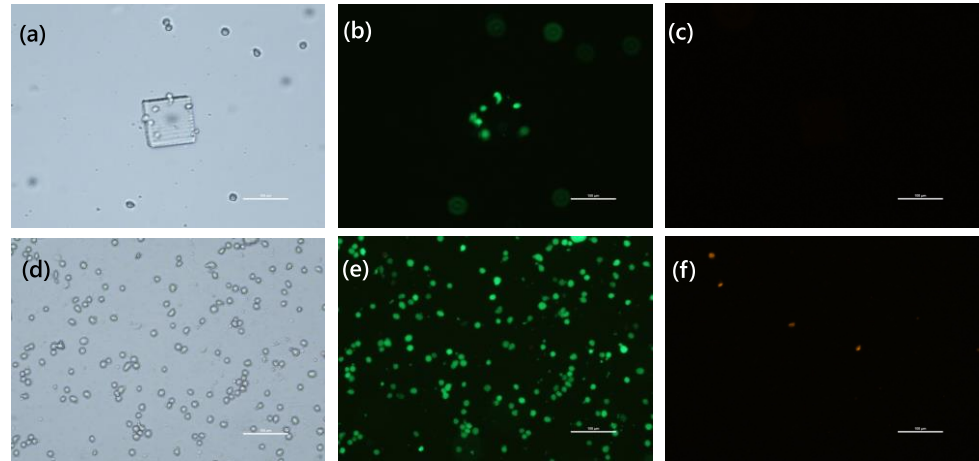


Figure 3. Microscopic images of HeLa cells stained with Calcein-AM and PI. (a–c) GelMA 5%w/v gel cured at 1200 mJ/cm². (d–f) Negative control. (a,d) Bright field images. (b,e) Green fluorescent images. (c,f) Red fluorescent images. Scale bars: 100 μm.

3.2. Biodegradability of GelMA

Figure 4a,b demonstrates the biodegradation of GelMA hydrogels with and without encapsulated cells after 5 days. The gel containing cells exhibited significant degradation, while the cell-free gel remained largely intact. While the cell-free gel showed a slight decrease in the area, it was not statistically significant.

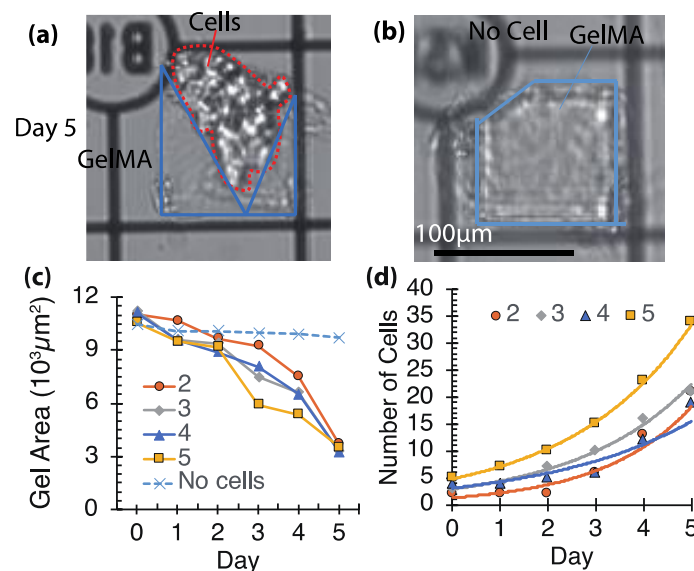


Figure 4. GelMA degradation and proliferation. Proliferation of cells in 5%w/v GelMA hydrogel with a size of 100 μm × 100 μm. (a) Images of cells on Day 5. The arrows in the figure indicate that HeLa cells and cell division were observed. Three cells were encapsulated in the gel on Day 0. (b) Gel degradation without cells on Day 5. (c) Time series gel area with/without cells. A square pattern of 100 μm × 100 μm was used for this experiment. (d) Increase in cell number from Day 0 to Day 5.

The change in the gel area over time was quantified to assess cell biodegradability (Figure 4c). A $100\ \mu\text{m} \times 100\ \mu\text{m}$ square pattern was used for light irradiation. The initial cell count, and the initial area of the cell-free gel are shown in the graph. The graph highlights a significant difference in the area between the initial cell-embedded gels and the cell-free gel. The rate of decrease in the area is related to time and is not strongly related to the initial cell count. This reason is explained by the fact that the number of cells in the hydrogels is comparable on Day 5. A significant decrease in the gel area occurred after Day 3, suggesting cell-mediated degradation. The area of the cell-free gel stabilized at approximately $10 \times 10^3\ \mu\text{m}^2$ by Day 5, while the area of the initial cell-embedded gels, averaged across four hydrogels, decreased to approximately $3.4 \pm 0.2 \times 10^3\ \mu\text{m}^2$.

Figure 4d examines cell proliferation within $100\ \mu\text{m} \times 100\ \mu\text{m}$ GelMA hydrogels after immobilization. Series 2–5 in the graph represent the initial number of encapsulated cells on Day 0. The cells within the gel continued to proliferate throughout the 5 days, reaching several dozen cells under all conditions by Day 5. The exponential growth curve observed resembles normal cell proliferation patterns [35].

3.3. Behavior of Cells Encapsulated in the GelMA Hydrogel

Figure 5a,b, respectively, presents observations of HeLa cells encapsulated in the GelMA hydrogel over 2 days with initial cell number of 3 and 5. In Figure 5a, a cell in the upper left corner exemplifies cell division occurring between Day 0 and Day 1, while the lower right corner shows cell division from Day 1 to Day 2. The hydrogel appears slightly deformed 2 days after cell division, suggesting some biodegradation by the cells.

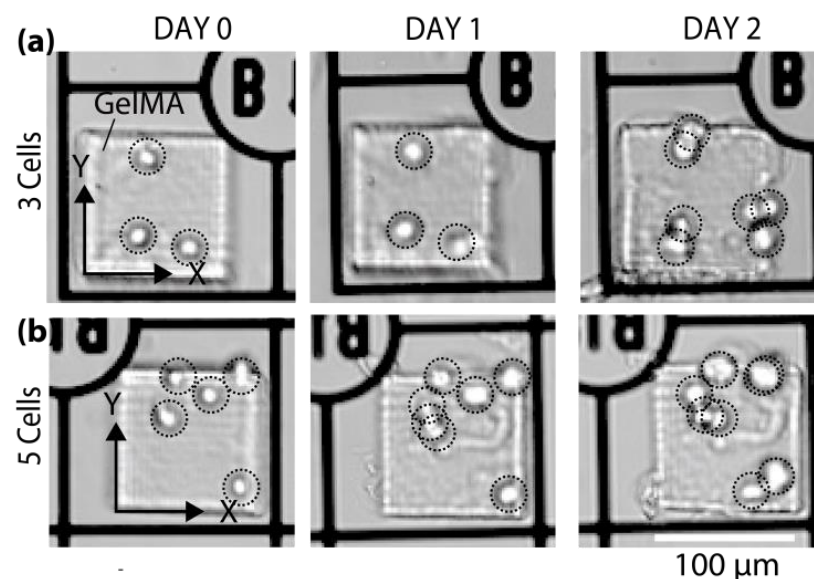


Figure 5. Time-lapse images of HeLa cells encapsulated in the GelMA hydrogel from Day 0 to Day 2. (a) Three cells and (b) five cells on Day 0, with single cells circled in black dashed lines.

Figure 6a–d depicts a graph tracing the coordinates of the hydrogel corners and encapsulated cells, with the origin at a grid intersection. Cells remained confined within the gel, even when encountering the edge, and tended to move inward. Figure 6e shows the measured displacement of cells from their initial positions. The average cell migration was $12.2\ \mu\text{m} \pm 7.6\ \mu\text{m}$ ($N = 14$) on Day 1 and $16.1 \pm 9.6\ \mu\text{m}$ ($N = 14$) on Day 2. A stiffer GelMA hydrogel might potentially reduce cell displacement, as reported in [36].

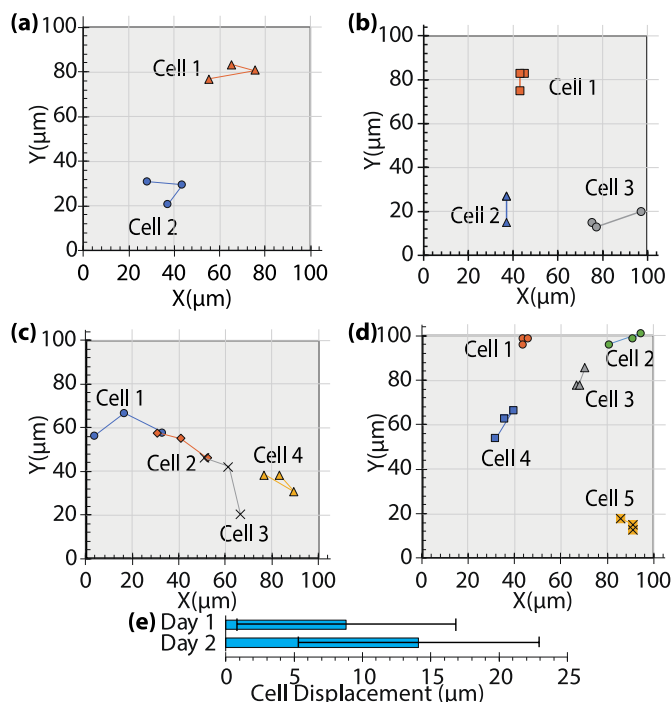


Figure 6. Motility analysis of HeLa cells encapsulated in GelMA hydrogel for 2 days. (a–d) Trajectories of cells with initial cell numbers ranging from 2 to 5. Gray areas indicate GelMA hydrogel. (e) Average cellular displacement on Day 1 and Day 2.

3.4. Recovery of Cells Encapsulated in GelMA

This study presents a novel technique for recovering adherent cells using a blue laser and DMD to photopolymerize a gel around individual cells. Patterned irradiation at 800 mJ/cm² selectively encapsulated HeLa cells in the GelMA hydrogel on a coverslip (Figure 7a). A subsequent 4 min trypsin treatment effectively removed unwanted cells, leaving only the encapsulated HeLa cells (Figure 7b). While longer trypsin exposure (10 min) did not fully degrade the gel, the desired cells remained encapsulated (Figure 7c). This method allows for the detachment of unwanted cells while specifically collecting the targeted cells.

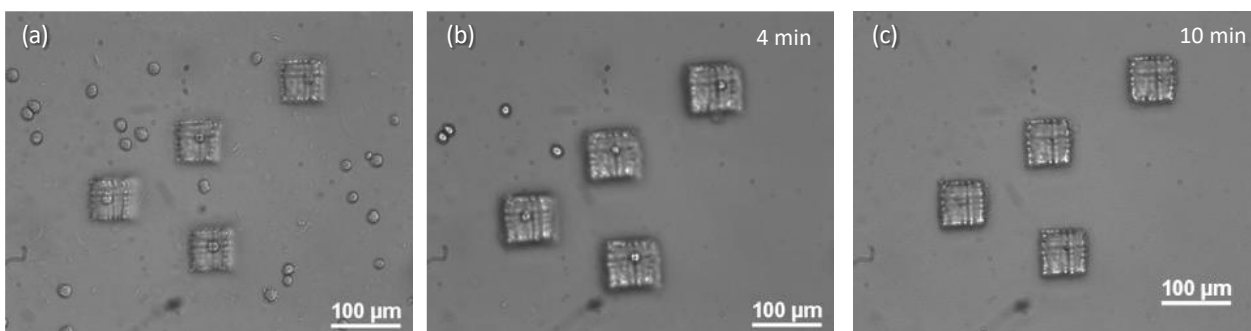


Figure 7. Collection of cells encapsulated in GelMA photocured at 800 mJ/cm² by trypsin treatment. (a) Immediately after irradiation. (b) Four min and (c) ten min after the addition of trypsin. The four cells remained trapped in the GelMA hydrogel.

For suspended cells, irradiation at 600 mJ/cm² resulted in HeLa cell encapsulation, but these cells were not readily detached by rinsing (Figure 8). Rinsing removed unwanted cells, and the encapsulated cells were subsequently collected by degrading the GelMA with trypsin. Video S1 further illustrates the gel dissolution process with trypsin and the release of cells from the GelMA hydrogels after 5 min of treatment.

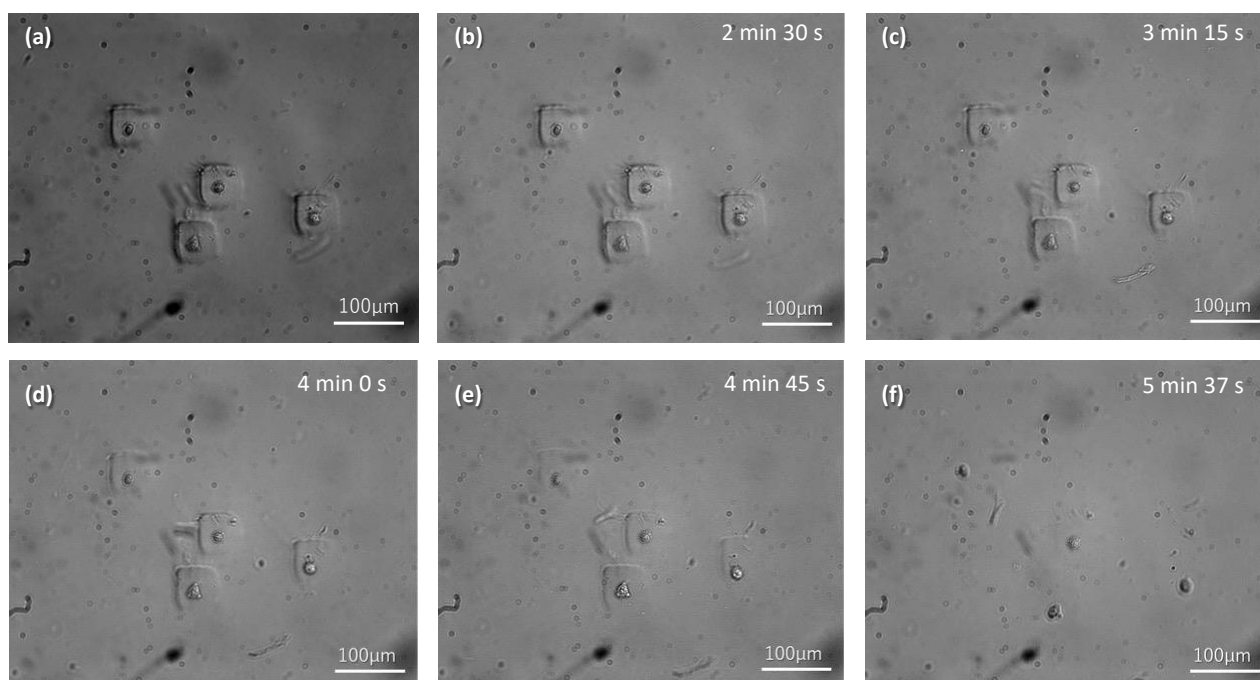


Figure 8. Dissolution of GelMA photocured at $600 \text{ mJ}/\text{cm}^2$ in trypsin and collection of the cells after the trypsin-induced degradation. (a) Immediately after the photopolymerization of GelMA. Trypsin treatment after (b) 2 min 30 s, (c) 3 min 15 s, (d) 4 min, (e) 4 min 45 s, and (f) 5 min 37 s.

This study chose GelMA over PEGDA due to its superior degradability with trypsin, as the degradation of PEGDA is more difficult [12–14]. PEGDA hydrogels primarily degrade via hydrolysis of the ester bonds, with degradation occurring more rapidly at an acidic or alkaline pH [37]. This property of PEGDA has made it challenging to collect live cells. In contrast, GelMA hydrogels degraded more readily than PEGDA hydrogels under mild enzymatic conditions. The hydrolytic degradation of PEGDA is a slow process compared to the enzymatic degradation of GelMA. Our approach takes advantage of the different properties inside and outside the GelMA hydrogels for targeted cell collection. Our results confirm that prolonged exposure to light increases the dissolution time of GelMA hydrogels, which is consistent with previous reports on the proteolytic degradation of GelMA hydrogels [28,29].

4. Conclusions

This study highlights the suitability of GelMA over PEGDA for cell encapsulation. The dimension and viability evaluations of GelMA photopolymerized with an integrated light intensity of $1000\text{--}2000 \text{ mJ}/\text{cm}^2$ showed similar pattern formation. Interestingly, HeLa cells encapsulated in $5\%w/v$ GelMA were better collected within a 2-day culture period due to GelMA's shape stability. Further demonstrating the biocompatibility of GelMA, HeLa cells within the gel exhibited exponential proliferation over 5 days. The gel area where cells were encapsulated significantly decreased after 5 days, suggesting biodegradation by the cells. The averaged cell displacement remained less than $20 \mu\text{m}$ from the initial position.

We demonstrated two targeted cell recovery strategies. (1) Adherent cells: Targeted adherent cells were fixed on the coverslip using $800 \text{ mJ}/\text{cm}^2$ light irradiation. Most unwanted cells detached within 4 min of trypsin treatment. After 10 min, only encapsulated cells remained, achieving the selective removal of unnecessary cells. (2) Floating cells: Only targeted floating cells were exposed to light and immobilized on a coverslip. After photoencapsulation, PBS(-) washes removed unwanted cells. Trypsin treatment (6 min) dissolved the polymerized gel at $600 \text{ mJ}/\text{cm}^2$, allowing for the collection of only the targeted cells.

This efficient cell recovery method can be integrated with the existing automated irradiation setup [31] and cell detection method [38] to further enhance targeted cell collection.

Supplementary Materials: The following supporting information can be downloaded at: <https://www.mdpi.com/article/10.3390/micro4020018/s1>; Video S1: Dissolution of GelMA hydrogels containing single cells with trypsin and the release of the cells from the hydrogels.

Author Contributions: Conceptualization, M.N.; methodology, V.K.P.S., T.F. and Y.S.; validation, V.K.P.S., T.F. and Y.S.; formal analysis, M.N.; investigation, M.N.; resources, T.F. and Y.S.; data curation, M.N.; writing—original draft preparation, V.K.P.S., T.F., Y.S. and M.N.; writing—review and editing, M.N., S.O., T.S. and T.S.S.; visualization, M.N.; supervision, T.S. and M.N.; project administration, M.N.; funding acquisition, M.N. All authors have read and agreed to the published version of the manuscript.

Funding: This work was supported by the Amano Institute of Technology (Hamamatsu, Japan) and MEXT/JSPS KAKENHI (grant numbers JP23H00168, JP20K20961, and JP20H02115).

Institutional Review Board Statement: Not applicable.

Data Availability Statement: The raw data supporting the conclusions of this article will be made available by the authors on request.

Conflicts of Interest: The authors declare no conflicts of interest.

References

1. Soo Kim, H.; Devarenne, T.P.; Han, A. A High-Throughput Microfluidic Single-Cell Screening Platform Capable of Selective Cell Extraction. *Lab. A Chip* **2015**, *15*, 2467–2475. [[CrossRef](#)] [[PubMed](#)]
2. Terekhov, S.S.; Smirnov, I.V.; Stepanova, A.V.; Bobik, T.V.; Mokrushina, Y.A.; Ponomarenko, N.A.; Belogurov, A.A.; Rubtsova, M.P.; Kartseva, O.V.; Gomzikova, M.O.; et al. Microfluidic Droplet Platform for Ultrahigh-Throughput Single-Cell Screening of Biodiversity. *Proc. Natl. Acad. Sci. USA* **2017**, *114*, 2550–2555. [[CrossRef](#)] [[PubMed](#)]
3. Segaliny, A.I.; Li, G.; Kong, L.; Ren, C.; Chen, X.; Wang, J.K.; Baltimore, D.; Wu, G.; Zhao, W. Functional TCR T Cell Screening Using Single-Cell Droplet Microfluidics. *Lab. A Chip* **2018**, *18*, 3733–3749. [[CrossRef](#)] [[PubMed](#)]
4. Müller, S.; Nebe-von-Caron, G. Functional Single-Cell Analyses: Flow Cytometry and Cell Sorting of Microbial Populations and Communities. *FEMS Microbiol. Rev.* **2010**, *34*, 554–587. [[CrossRef](#)] [[PubMed](#)]
5. Wilkerson, M.J. Principles and Applications of Flow Cytometry and Cell Sorting in Companion Animal Medicine. *Vet. Clin. Small Anim. Pract.* **2012**, *42*, 53–71. [[CrossRef](#)] [[PubMed](#)]
6. Adan, A.; Alizada, G.; Kiraz, Y.; Baran, Y.; Nalbant, A. Flow Cytometry: Basic Principles and Applications. *Crit. Rev. Biotechnol.* **2017**, *37*, 163–176. [[CrossRef](#)]
7. McKinnon, K.M. Flow Cytometry: An Overview. *Curr. Protoc. Immunol.* **2018**, *120*, 5.1.1–5.1.11. [[CrossRef](#)] [[PubMed](#)]
8. LaBelle, C.A.; Massaro, A.; Cortés-Llanos, B.; Sims, C.E.; Allbritton, N.L. Image-Based Live Cell Sorting. *Trends Biotechnol.* **2021**, *39*, 613–623. [[CrossRef](#)] [[PubMed](#)]
9. Lu, Z.; Moraes, C.; Ye, G.; Simmons, C.A.; Sun, Y. Single Cell Deposition and Patterning with a Robotic System. *PLoS ONE* **2010**, *5*, e13542. [[CrossRef](#)]
10. Nagai, M.; Kato, K.; Oohara, K.; Shibata, T. Pick-and-Place Operation of Single Cell Using Optical and Electrical Measurements for Robust Manipulation. *Micromachines* **2017**, *8*, 350. [[CrossRef](#)]
11. Chen, B.; Lim, S.; Kannan, A.; Alford, S.C.; Sunden, F.; Herschlag, D.; Dimov, I.K.; Baer, T.M.; Cochran, J.R. High-Throughput Analysis and Protein Engineering Using Microcapillary Arrays. *Nat. Chem. Biol.* **2016**, *12*, 76–81. [[CrossRef](#)] [[PubMed](#)]
12. Negishi, R.; Takai, K.; Tanaka, T.; Matsunaga, T.; Yoshino, T. High-Throughput Manipulation of Circulating Tumor Cells Using a Multiple Single-Cell Encapsulation System with a Digital Micromirror Device. *Anal. Chem.* **2018**, *90*, 9734–9741. [[CrossRef](#)] [[PubMed](#)]
13. Negishi, R.; Iwata, R.; Tanaka, T.; Kisailus, D.; Maeda, Y.; Matsunaga, T.; Yoshino, T. Gel-Based Cell Manipulation Method for Isolation and Genotyping of Single-Adherent Cells. *Analyst* **2019**, *144*, 990–996. [[CrossRef](#)] [[PubMed](#)]
14. Negishi, R.; Saito, H.; Iwata, R.; Tanaka, T.; Yoshino, T. Performance Evaluation of a High-Throughput Separation System for Circulating Tumor Cells Based on Microcavity Array. *Eng. Life Sci.* **2020**, *20*, 485–493. [[CrossRef](#)] [[PubMed](#)]
15. Sun, T.; Kovac, J.; Voldman, J. Image-Based Single-Cell Sorting via Dual-Photopolymerized Microwell Arrays. *Anal. Chem.* **2014**, *86*, 977–981. [[CrossRef](#)] [[PubMed](#)]
16. Browning, M.B.; Cereceres, S.N.; Luong, P.T.; Cosgriff-Hernandez, E.M. Determination of the in Vivo Degradation Mechanism of PEGDA Hydrogels. *J. Biomed. Mater. Res. Part A* **2014**, *102*, 4244–4251. [[CrossRef](#)]
17. Perera, D.; Medini, M.; Seethamraju, D.; Falkowski, R.; White, K.; Olabisi, R.M. The Effect of Polymer Molecular Weight and Cell Seeding Density on Viability of Cells Entrapped within PEGDA Hydrogel Microspheres. *J. Microencapsul.* **2018**, *35*, 475–481. [[CrossRef](#)] [[PubMed](#)]

18. Nagai, M.; Kato, K.; Shibata, T. Integration of Microorganism *Vorticella Convallaria* and Poly (Ethylene Glycol) Diacrylate Hydrogel for Biohybrid Systems. *Mech. Eng. Lett.* **2016**, *2*, 16–00445. [[CrossRef](#)]
19. Yue, K.; Trujillo-de Santiago, G.; Alvarez, M.M.; Tamayol, A.; Annabi, N.; Khademhosseini, A. Synthesis, Properties, and Biomedical Applications of Gelatin Methacryloyl (GelMA) Hydrogels. *Biomaterials* **2015**, *73*, 254–271. [[CrossRef](#)]
20. Piao, Y.; You, H.; Xu, T.; Bei, H.-P.; Piwko, I.Z.; Kwan, Y.Y.; Zhao, X. Biomedical Applications of Gelatin Methacryloyl Hydrogels. *Eng. Regen.* **2021**, *2*, 47–56. [[CrossRef](#)]
21. Ghosh, R.N.; Thomas, J.; Vaidehi, B.R.; Devi, N.G.; Janardanan, A.; Namboothiri, P.K.; Peter, M. An Insight into Synthesis, Properties and Applications of Gelatin Methacryloyl Hydrogel for 3D Bioprinting. *Mater. Adv.* **2023**, *4*, 5496–5529. [[CrossRef](#)]
22. Cui, J.; Wang, H.; Shi, Q.; Sun, T.; Huang, Q.; Fukuda, T. Multicellular Co-Culture in Three-Dimensional Gelatin Methacryloyl Hydrogels for Liver Tissue Engineering. *Molecules* **2019**, *24*, 1762. [[CrossRef](#)]
23. Zhao, X.; Liu, S.; Yildirim, L.; Zhao, H.; Ding, R.; Wang, H.; Cui, W.; Weitz, D. Injectable Stem Cell-Laden Photocrosslinkable Microspheres Fabricated Using Microfluidics for Rapid Generation of Osteogenic Tissue Constructs. *Adv. Funct. Mater.* **2016**, *26*, 2809–2819. [[CrossRef](#)]
24. Wang, H.; Liu, H.; Liu, H.; Su, W.; Chen, W.; Qin, J. One-Step Generation of Core–Shell Gelatin Methacrylate (GelMA) Microgels Using a Droplet Microfluidic System. *Adv. Mater. Technol.* **2019**, *4*, 1800632. [[CrossRef](#)]
25. Gao, X.; Hu, X.; Yang, D.; Hu, Q.; Zheng, J.; Zhao, S.; Zhu, C.; Xiao, X.; Yang, Y. Acoustic Quasi-Periodic Bioassembly Based Diverse Stem Cell Arrangements for Differentiation Guidance. *Lab. Chip* **2023**, *23*, 4413–4421. [[CrossRef](#)] [[PubMed](#)]
26. Hu, Q.; Hu, X.; Shi, Y.; Liang, L.; Zhu, J.; Zhao, S.; Wang, Y.; Wu, Z.; Wang, F.; Zhou, F.; et al. Heterogeneous Tissue Construction by On-Demand Bubble-Assisted Acoustic Patterning. *Lab. Chip* **2023**, *23*, 2206–2216. [[CrossRef](#)]
27. Hu, X.; Zhao, S.; Luo, Z.; Zuo, Y.; Wang, F.; Zhu, J.; Chen, L.; Yang, D.; Zheng, Y.; Zheng, Y.; et al. On-Chip Hydrogel Arrays Individually Encapsulating Acoustic Formed Multicellular Aggregates for High Throughput Drug Testing. *Lab. Chip* **2020**, *20*, 2228–2236. [[CrossRef](#)]
28. Chansoria, P.; Asif, S.; Polkoff, K.; Chung, J.; Piedrahita, J.A.; Shirwaiker, R.A. Characterizing the Effects of Synergistic Thermal and Photo-Cross-Linking during Biofabrication on the Structural and Functional Properties of Gelatin Methacryloyl (GelMA) Hydrogels. *ACS Biomater. Sci. Eng.* **2021**, *7*, 5175–5188. [[CrossRef](#)]
29. Kulkarni, N.S.; Chauhan, G.; Goyal, M.; Sarvepalli, S.; Gupta, V. Development of Gelatin Methacrylate (GelMa) Hydrogels for Versatile Intracavitary Applications. *Biomater. Sci.* **2022**, *10*, 4492–4507. [[CrossRef](#)]
30. Allen, N.B.; Abar, B.; Johnson, L.; Burbano, J.; Danilkowicz, R.M.; Adams, S.B. 3D-Bioprinted GelMA-Gelatin-Hydroxyapatite Osteoblast-Laden Composite Hydrogels for Bone Tissue Engineering. *Bioprinting* **2022**, *26*, e00196. [[CrossRef](#)]
31. Selvam, V.K.P.; Kamaludin, M.L.A.B.; Murtaza, G.; Chowdhury, R.H.; Debnath, T.; Okamoto, S.; Shibata, T.; Santra, T.S.; Nagai, M. Image-Based Gel Encapsulation of Suspended Single Cells for Parallel Single-Cell Screening. *J. Robot. Mechatron.* **2023**, *35*, 1177–1184. [[CrossRef](#)]
32. Yin, J.; Yan, M.; Wang, Y.; Fu, J.; Suo, H. 3D Bioprinting of Low-Concentration Cell-Laden Gelatin Methacrylate (GelMA) Bioinks with a Two-Step Cross-Linking Strategy. *ACS Appl. Mater. Interfaces* **2018**, *10*, 6849–6857. [[CrossRef](#)] [[PubMed](#)]
33. Pahoff, S.; Meinert, C.; Bas, O.; Nguyen, L.; Klein, T.J.; Huttmacher, D.W. Effect of Gelatin Source and Photoinitiator Type on Chondrocyte Redifferentiation in Gelatin Methacryloyl-Based Tissue-Engineered Cartilage Constructs. *J. Mater. Chem. B* **2019**, *7*, 1761–1772. [[CrossRef](#)] [[PubMed](#)]
34. Nagai, M.; Sato, S.; Hiratsuka, S.; Kawaharada, S.; Okamoto, S.; Santra, T.S.; Shibata, T. Parallel Photothermal Coalescence of Biocompatible Photocurable PEGDA Droplets. *IEEJ Trans. Sens. Micromachines* **2023**, *143*, 49–54. [[CrossRef](#)]
35. Verma, A.; Verma, M.; Singh, A. Chapter 14-Animal Tissue Culture Principles and Applications. In *Animal Biotechnology*, 2nd ed.; Verma, A.S., Singh, A., Eds.; Academic Press: Boston, UK, 2020; pp. 269–293. ISBN 978-0-12-811710-1.
36. Vasudevan, J.; Lim, C.T.; Fernandez, J.G. Cell Migration and Breast Cancer Metastasis in Biomimetic Extracellular Matrices with Independently Tunable Stiffness. *Adv. Funct. Mater.* **2020**, *30*, 2005383. [[CrossRef](#)]
37. Stillman, Z.; Jarai, B.M.; Raman, N.; Patel, P.; Fromen, C.A. Degradation Profiles of Poly(Ethylene Glycol)Diacrylate (PEGDA)-Based Hydrogel Nanoparticles. *Polym. Chem.* **2020**, *11*, 568–580. [[CrossRef](#)]
38. Debnath, T.; Hattori, R.; Okamoto, S.; Shibata, T.; Santra, T.S.; Nagai, M. Automated Detection of Patterned Single-Cells within Hydrogel Using Deep Learning. *Sci. Rep.* **2022**, *12*, 18343. [[CrossRef](#)]

Disclaimer/Publisher’s Note: The statements, opinions and data contained in all publications are solely those of the individual author(s) and contributor(s) and not of MDPI and/or the editor(s). MDPI and/or the editor(s) disclaim responsibility for any injury to people or property resulting from any ideas, methods, instructions or products referred to in the content.